Apoptosis (2010) 15:488–498
DOI 10.1007/s10495-009-0439-2

ORIGINAL PAPER

A PKC-β inhibitor protects against cardiac microvascular ischemia reperfusion injury in diabetic rats

Liping Wei · Dongdong Sun · Zhiyong Yin · Yuan Yuan · Andrew Hwang · Yingmei Zhang · Rui Si · Rongqing Zhang · Wenyi Guo · Feng Cao · Haichang Wang

Published online: 1 January 2010

Abstract PKC-β inhibitor Ruboxistaurin (RBX or LY333531) can be used to reverse diabetic microvascular complication. However, it has not been previously established whether RBX can protect against ischemia/reperfusion (I/R) injury of cardiac microvessels in diabetic rats. STZ-induced diabetic rats were randomized into four groups and underwent I/R procedures. Cardiac barrier function and the region of cardiac microvascular lesion were examined. Cell monolayer barrier function was detected in cultured cardiac microvascular endothelial cells (CMECs) subjected to simulated I/R (SI/R). PKC-β siRNA was transfected into CMECs to silence PKC-β. Apoptosis Index of CMECs was detected by TUNEL assay and phosphor-LIMK2 protein expression was examined by Western blot analysis. RBX and insulin administration significantly reduced the cardiac microvascular lesion region and Apoptosis Index of endothelial cells (all $P < 0.05$ vs. no-treatment group). RBX decreased phosphor-LIMK2 expression ($P < 0.05$ vs. no-treatment group). RBX pretreatment and transfection with PKC-β siRNA induced a rapid barrier enhancement in CMECs monolayer as detected by increased transendothelial electrical resistance (TER) and decreased FITC-dextran clearance (all $P < 0.05$ vs. no-treatment group). Meanwhile, RBX pretreatment and transfection with PKC-β siRNA significantly decreased TUNEL positive CMECs and phosphor-LIMK2 expression in cultured CMECs (all $P < 0.05$ vs. no-treatment group). RBX pretreatment reduced F-actin/G-actin in cultured CMECs, reproducing the same effect as PKC-β siRNA. These data indicate that PKC-β inhibitor (RBX) may be helpful in attenuating the risk of severe cardiac microvascular I/R injury in diabetic rats partly due to its maintenance of endothelial barrier function and anti-apoptotic effect.

Keywords Hyperglycemia · PKC-β · Cardiac microvascular endothelial cells · Ischemia/reperfusion · Apoptosis · Permeability

Liping Wei, Dongdong Sun and Zhiyong Yin contributed equally to this work.

L. Wei · D. Sun · Z. Yin · Y. Yuan · Y. Zhang · R. Si · R. Zhang · W. Guo · F. Cao (✉) · H. Wang (✉)
Department of Cardiology, Xijing Hospital, Fourth Military Medical University, 710032 Xi'an, Shaanxi, China
e-mail: wind8828@gmail.com

H. Wang
e-mail: wanghc@fmmu.edu.cn

L. Wei
Tianjin Union Medicine Center, 300121 Tianjin, China

A. Hwang
Department of Radiology, Molecular Imaging Program of Stanford, Stanford University, Stanford, CA, USA

Introduction

The incidence of coronary heart disease and stroke in diabetic patients has gradually increased in recent years [1]. In those patients who have undergone revascularization, reperfusion injury is common [2]. Diabetic hearts are more sensitive to ischemic injury than the hearts of non-diabetics [3, 4]. Myocardial salvage after reperfusion may be limited by deleterious changes in the microcirculation of the previously ischemic tissue [5]. Endothelial barrier dysfunction is considered to be one of the initiating mechanisms underlying the pathogenesis of diabetic

microvascular complication [6]. Characteristic changes in endothelial barrier dysfunction during the early stages of diabetes include autoregulatory dysfunction and increased endothelial permeability [7, 8]. These pathologic and physiologic reactions all contribute to aggravating microvascular lesion and apoptosis of endothelial cell. Scarabelli et al. [9] reported that in isolated perfused heart subjected to ischemia and reperfusion, endothelial apoptosis occured at an earlier time point than that of cardiomyocytes. Therefore, function and integrity of endothelial cells probably play more important role in ischemia reperfusion injury in diabetes.

In addition, maintenance of normal barrier function or endothelial permeability relies on the dynamic balance between adhesive and centripetal forces of cells. Amounts of previous researches demonstrated protein kinase C (PKC) activation was involved in changes in adhesive force, resulting in damage to normal barrier function [10, 11]. LIM Kinase 2 plays an important role in controlling the morphology and function of the cytoskeleton, which correlates maintenance of normal centripetal force [12]. So PKC and LIM Kinase 2, respectively, modulate the two maintenance factors of normal barrier function in endothelial cells.

Hyperglycemia can result in severe microvascular barrier dysfunction through subsequent activation of PKC isoforms in diabetes [6, 10, 13]. Protein kinases Cs (PKCs) belong to a family of serine/threonine kinases that participate in vascular cell signal transduction. The individual isoforms of PKCs respond differently to hyperglycemia, however, both experiments in vivo and in vitro support the predominant role of PKC-β in diabetic microvascular complications especially in heart and aorta [14, 15]. Many studies have shown that RBX, a highly selective PKC-β inhibitor, normalizes endothelial function, improves renal glomerular filtration rate and prevents loss of visual acuity in diabetic patients [16, 17]. However, it has not been previously established whether administration of a PKC-β inhibitor provides protection against ischemia reperfusion (I/R) injury of cardiac microvessels in diabetes. In addition, previous studies [18, 19] reported insulin can significantly reduce myocardial and endothelial injury in rats suffering an ischemic insult.

We therefore designed experiments to (1) determine whether cardiac microvascular barrier dysfunction and Apoptosis Index of cardiac microvascular endothelial cells (CMECs) was increased in diabetic rats subjected to I/R; (2) elucidate whether RBX can improve cardiac microvascular barrier function during I/R and compared this protective effect with insulin; and (3) investigate the mechanism(s) by which RBX may modulate I/R injury in CMECs interfered by high glucose or diabetic states.

Methods

Animal preparation for in vivo experiments

All animal procedures were performed in accordance with protocols approved by the Fourth Military Medical University Animal Research Committee and international research animal care guidelines. 40 male Sprague–Dawley diabetic rats (weight 250–280 g) were induced by a single intraperitoneal injection of streptozotocin (STZ, 50 mg/kg in 0.9% saline, Sigma, USA). Blood glucose levels were measured 1 week after STZ injection. Animals with glucose levels equal to or more than 16.6 mmol/L were classified as diabetes. The diabetic rats were randomized into 4 groups: (1) Sham group ($n = 10$); (2) I/R group: without any treatment ($n = 10$); (3) RBX + I/R group ($n = 10$): administered orally with ruboxistaurin (Lilly, USA) at a dose of 5 mg/kg/day for 2 weeks; (4) Insulin + I/R group ($n = 10$): subcutaneously injected with insulin at a dose of 0.5 U/kg/d for 2 weeks. Animals received different pretreatment before surgery. The experimental model of I/R was accomplished by exteriorizing the heart via a left thoracic incision and placing a 6-0 silk suture slipknot around the left anterior descending coronary artery (LAD). After 30 min of ischemia, the slipknot was released, and the myocardium was reperfused for 72 h. Sham-operated rats ($n = 10$) underwent the same surgical procedures except that the suture placed under the LAD was not tightened.

Examination of cardiac microvascular barrier function

Lanthanum nitrate is a reagent that has been used in a number of studies to test barrier function of endothelial cells [20]. Under healthy conditions, lanthanum nitrate is unable to traverse endothelial cell-to-cell junctions in significant quantities, but when such barriers are deficient as in pathologic conditions it may cross cell boundaries via paracellular diffusion. Hearts of anaesthetized rats were isolated and perfused via the carotid artery with 50 mL of prefixative solution (100 mM Tris, pH 7.2, 150 mM NaCl, 5.6 mM KCl, 1 mM MgCl2, 2.5 mM CaCl2, 3.7 mM glucose and 3.6 mM procaine) followed by 250 mL of fixing solution (2.5% glutaraldehyde and 2% paraformaldehyde in 0.1 M sodium cacodylate buffer, pH 7.2, containing 2% lanthanum nitrate) using a peristaltic pump. The perfusion pressure was monitored with a mercury manometer and maintained at 100 mm Hg. After perfusion, the hearts were kept in the same fixative without lanthanum for 1 h. The samples were then rinsed in washing solution (0.15 M NaCl plus 0.2 M sucrose). Ultra-thin sections (60 nm thick) were cut, mounted on copper grids (200 mesh)

and examined under a transmission electron microscope (JEM-2000EX, Japan).

Determination of cardiac microvascular lesion region

After 30 min ischemia and 72 h reperfusion, the hearts were harvested and subjected to the cardiac microvascular lesion determination as previous described [21]. In brief, thioflavin S (Sigma, USA) at 1 mL/kg of a 4% solution in PBS was injected into the heart to identify the region of cardiac microvascular lesion. Thioflavin S is a fluorescent green-yellow dye that stains the endothelium and serves as a marker of perfusion and therefore is a standard marker for identifying zones of cardiac microvascular lesion. The coronary artery was re-occluded and 4 mL of a 50% solution of Unisperse blue dye was injected into the left atrium. The ischemic risk region was delineated by use of Unisperse blue dye. The heart was sliced transversely into six to eight sections and photographed under ultraviolet light to identify the region of cardiac microvascular lesion. The microvascular lesion area was expressed as a percentage of the Hypofluorescent area/(LV-Unisperse blue staining area).

Isolation of cardiac microvascular endothelial cells (CMECs) for in vitro experiments

Left ventricles of rats were harvested and minced into 1 mm^3 small pieces after removal of the endocardial endothelium and the epicardial coronaries from male Sprague–Dawley rats weighing 100–120 g. The tissue pieces were dissociated by collagenase II (1 mg/mL, Invitrogen, USA) and subsequently cultured in Endothelial Growth Medium consisting of defined growth factors and supplemented with additional FBS up to 15% final concentration. Passage 3–5 cells were used for further studies. The cells were identified by staining with 15 μg Alexa Fluor 594 AcLDL (Molecular Probes, USA) overnight at 37°C and staining with CD31(Chemicon, USA). RBX (Alexis, USA) was dissolved in dimethyl sulfoxide (DMSO) (Sigma, USA) to a final concentration of 10 nmol/L. Afterwards, CMECs were cultured in different mediums including high glucose medium (25 mmol), high glucose plus RBX (10 nmol/L) medium and CMECs transfected with PKC-β siRNA. CMECs were subjected to 30 min of simulated ischemia and 2 h of reperfusion (SI/R) as described in previous studies [18].

Transfection of PKC-β siRNA into CMECs

Transfections were performed with EntransterTM-R (Engreen Biosystem, China) according to the manufacturer's instructions. PKC-β specific siRNAs were synthesized (Santa Cruz, USA) and used for transfecting. The sense and antisense strands of the PKC-β siRNA were GUCAGAUGCUGAUGUUCCUUU and UUCAGUCUAC GACUACAAGGA. CMECs were transfected after 48 h of culture. EntransterTMR in transfection reagent (8 μL) was added to 100 μL OptiMEM serum-free medium containing 2 nmol/L of each siRNA oligo, incubated for 10 min, and added to the 6-cm plate containing 2 mL medium. The efficacy of PKC-β silencing and reductions in protein expression was assessed after 72 h in the same group of cells by Western blot analysis.

Assessment of apoptosis of CMECs in vivo and in vitro

The myocardial tissue was collected after 30 min ischemia and 72 h reperfusion. Apoptosis was detected by terminal deoxy-nucleotidyl transferase-mediated dUTP nick end-labeling (TUNEL, in green) assay using a Cell Death Detection Kit (Promaga, USA) according to the manufacturer's instructions. For double-labeling, the tissue sections were incubated with the red fluorescently-labeled monoclonal antibody against CD31 (Chemicon, USA) after incubation with TUNEL reaction mixture. For detection of total nuclei, the slides were covered with the mounting medium containing DAPI. The cultured CMECs after SI/R were collected to determine apoptotic cells using the TUNEL staining and detect total nuclei with DAPI. At least 6 slides per block were evaluated. Apoptosis Index (AI), i.e., the number of TUNEL-positive CMECs divided by the total CMECs per field, was determined.

Measurement of transendothelial electrical resistance (TER) and permeability of CMECs monolayer

Transendothelial electrical resistance (TER) is a measure of the ionic conductance of endothelial cells and can be used to assess junctional function [22]. TER increases when endothelial cells adhere and spread out, and decreases when endothelial cells retract or lose adhesion. Within In Vitro Vascular Permeability Assay kit (ECM640, Millipore, USA), CMECs at 100,000 cells/insert were seeded onto collagen coated inserts. After confluence, the cells were subjected SI/R, an electrical endothelial resistance system (Millipore, USA) was used to measure TER as previously described [23]. Confluence of CMECs monolayer was assessed as stabilized basal resistance of 800 Ω.

FITC-Dextran clearance was measured to assess changes in endothelial permeability. FITC-Dextran (final concentration 1 mg/mL) was added on top of the inserts, allowing it to permeate through the cell monolayer. The extent of permeability after 2 h was determined by using a fluorescent plate reader (Bio-Rad, USA) to measure the FITC content remaining on the plate.

Detection of phosphor-LIMK2 expression

To locate phosphor-LIMK2 expression in ischemic heart tissue, immunohistochemical staining was performed. Paraformaldehyde-fixed heart tissue was cut into semithin sections 4–5 μm thick, and stained with an antibody against phosphor-LIMK2 (1:250, Santa Cruz, USA). An IX71 cofocal microscope (Olympus, Japan) was used to examine the images.

Proteins from ischemic heart tissue and cultured CMECs were collected to perform Western blot analysis. Protein homogenates were separated on SDS–PAGE gels, transferred to nitrocellulose membranes, and Western blotting with monoclonal antibody against phosphor-LIMK2 (1:1,000, Santa Cruz, USA) were performed. Nitrocellulose membranes were then incubated with second antibodies for 1 h and the blot was developed with a Supersignal chemiluminescence detection kit (Pierce, USA). Immunoblotting was visualized with an Image Station 400 (Kodak, Japan).

Examination of F-actin content

Cultured CMECs were fixed in 4% formaldehyde and permeabilized with 0.2% triton X-100. Filamentous actin (F-actin) was stained with FITC-phalloidin (1:100, ALEXIS, USA). Free globular actin (G-actin) and (F-actin) content were examined using a commercially available assay kit (Cytoskeleton, USA).

Statistical analysis

All values were presented as mean ± SD (of n independent experiments). All data (except Western blot density) were compared by ANOVA followed by Bonferroni correction for post hoc analysis. P values of <0.05 were considered statistically significant. All of the statistical tests were performed using GraphPad Prism software version 5.0 (GraphPad Software, San Diego,CA). Graph of TER was performed using Sigmaplot 8.0 software (SPSS Inc, Chicago, USA).

Results

Metabolic characteristics of the diabetic rats in different experimental groups are shown in Table 1. These data displayed characteristic of diabetic condition produced by STZ and diabetic rats exhibited hyperglycemia and reduced body weight gain. RBX administration (21.4 ± 2.2 mmol/L vs. 22.3 ± 1.9 mmol/L, $P \geq 0.05$) did not influence glycemia but insulin treatment (15.3 ± 2.1 mmol/L vs. 21.2.5 ± 2.3 mmol/L, $P \leq 0.05$) decreased glycemia. Body weight slightly decreased in the RBX treatment group (271.6 ± 8.9 g vs. 243.5 ± 8.6 g, $P \leq 0.05$) and the no-treatment group (276.3 ± 9.6 vs. 230.5 ± 7.9, $P \leq 0.05$).

RBX pretreatment protects against cardiac microvascular injury in diabetic hearts after I/R

Extracellular tracer lanthanum nitrate was highlighted with arrows (Fig. 1, Upper panel). Minimal lanthanum traversed the endothelium in sham operation group (Fig. 1a). Severe disturbances of endothelium, edema and vacuolus were represented in diabetic rats subjected to I/R (Fig. 1b). In contrast, RBX pretreatment attenuated this severe pathology, with minimal lanthanum traversing the endothelium and without edema or vacuoles (Fig. 1c). We also observed protective role in insulin-treated diabetic hearts, with minimal lanthanum traversing the endothelium and edema presented (Fig. 1d).

The green fluorescence covered area indicates that successful reperfusion occurred. Hypofluorescent zones with arrow highlighted indicated the demarcation region of cardiac microvascular lesion, blue dye unstaining area indicated anatomic region of LAD dominated (Fig. 1, Lower panel). The microvascular lesion area averaged 0, 20.0 ± 1.7, 16.4 ± 1.9 and 15.9 ± 1.8% in the various groups, respectively. The region of cardiac microvascular lesion in no-treatment rats significantly increased and pretreatment with RBX (20.0 ± 1.7 vs. 16.4 ± 1.9%, $P \leq 0.05$) and insulin (20.0 ± 1.7 vs. 15.9 ± 1.8%, $P \leq 0.05$) reduced the cardiac microvascular lesion region,

Table 1 Metabolic characteristics of the diabetic rats in different experiment groups

Experiment groups	Experiment beginning		Experiment end	
	Weight (g)	Blood glucose (mmol/L)	Weight (g)	Blood glucose (mmol/L)
DM	276.3 ± 9.6	22.3 ± 1.9	230.5 ± 7.9*	21.4 ± 2.2
DM + RBX	271.6 ± 8.9	21.9 ± 1.7	243.5 ± 8.6$^{\#}$	19.5 ± 1.9
DM + Insulin	279.2 ± 10.2	21.2 ± 2.3	272.3 ± 9.8	15.3 ± 2.1**

Data are mean ± SD ($n = 6$), * $P < 0.05$ vs. experiment beginning of DM group, $^{\#}$ $P < 0.05$ vs. experiment beginning of RBX treatment group, ** $P < 0.01$ vs. experiment beginning of DM group

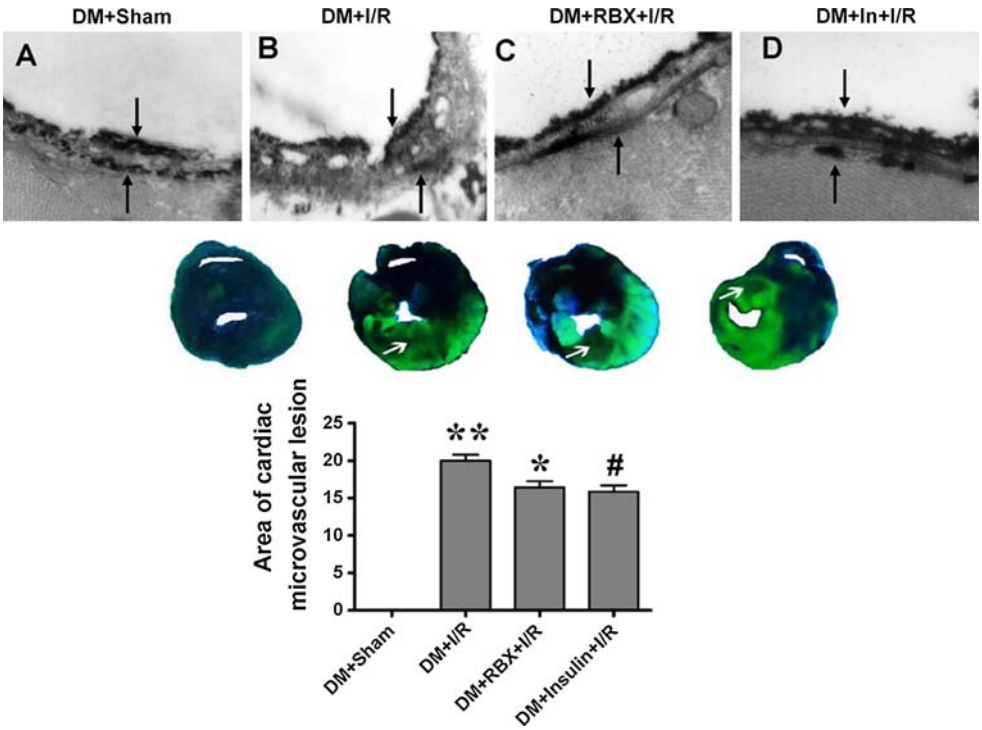

Fig. 1 Cardiac microvascular barrier function and microvascular lesion region in diabetic rats subjected to sham operation or ischemia reperfusion and receiving different treatments. Cardiac barrier function observed under transmission electron microscope (TEM) with Lanthanum nitrate as a tracer (*Upper panel*). The extracellular tracer lanthanum nitrate is highlighted with arrows. *Scale bar* represents 2 μm. Hypofluorescent area and Unisperse blue staining area were digitally measured (*Lower panel*). The microvascular lesion area was expressed as a percentage of the hypofluorescent area relative to (LV-Unisperse blue staining area) ($n = 8$). Values presented are means ± SEM. ** $P < 0.01$ vs. DM + Sham, * $P < 0.05$ vs. DM + I/R, $^{\#}$ $P < 0.05$ vs. DM + I/R

however, there are no significant differences between RBX and insulin pretreatment.

RBX pretreatment reduced Apoptosis Index of CMECs in diabetic hearts after I/R

Apoptosis of CMECs was detected by TUNEL assay and CD31 was used to locate CMECs distinguished from cardiomyocyte (Fig. 2). CMECs from sham operated hearts exhibited very low levels on the Apoptosis Index (AI) (4.21 ± 0.96%). In contrast, AI of CMECs significantly increased after diabetic hearts was subjected to I/R (4.21 ± 0.96 vs. 12.67 ± 2.21%, $P < 0.01$). Most notably, AI of CMECs in the heart of RBX (9.53 ± 1.48 vs. 12.67 ± 2.21%, $P \leq 0.05$) and insulin (8.95 ± 1.74 vs. 12.67 ± 2.21%, $P \leq 0.05$) pretreatment groups significantly decreased compared with diabetic hearts without treatment subjected to I/R.

RBX pretreatment downregulated phosphor-LIMK2 expression in diabetic heart after I/R

Phosphor-LIMK2 signal was significantly augmented in diabetics subjected to I/R compared to the sham operation group (Fig. 3a, b). When RBX was administered, phosphor-LIMK2 expression was significantly attenuated (Fig. 3c), however, insulin pretreatment did not influence phosphor-LIMK2 expression (Fig. 3d). Same results were found in Western blot analysis. Relative expression of phosphor-LIMK2 in diabetic heart subjected to I/R increased compared with that in the sham operation group (1.01 ± 0.10 vs. 0.66 ± 0.11, $P < 0.01$). Phosphor-LIMK2 expression was significantly downregulated by RBX administration (1.01 ± 0.10 vs. 0.76 ± 0.08, $P < 0.05$), however, insulin pretreatment did not attenuate phosphor-LIMK2 expression (1.01 ± 0.10 vs. 0.96 ± 0.13, $P \geq 0.05$) (Fig. 3e).

RBX pretreatment reduced Apoptosis Index of CMECs after SI/R

CMECs were successful cultured and identified. Confluence shape (Fig. 4a) and the typical staining of CMECs were shown. Cells exhibited intense cytoplasmic staining (in red) that was DiL-aLDL (Fig. 4b). A positive staining reaction CD31 antibody was determined by the presence of green fluorescence of the FITC-secondary antibody (Invitrogen, USA) conjugates after excitation by the

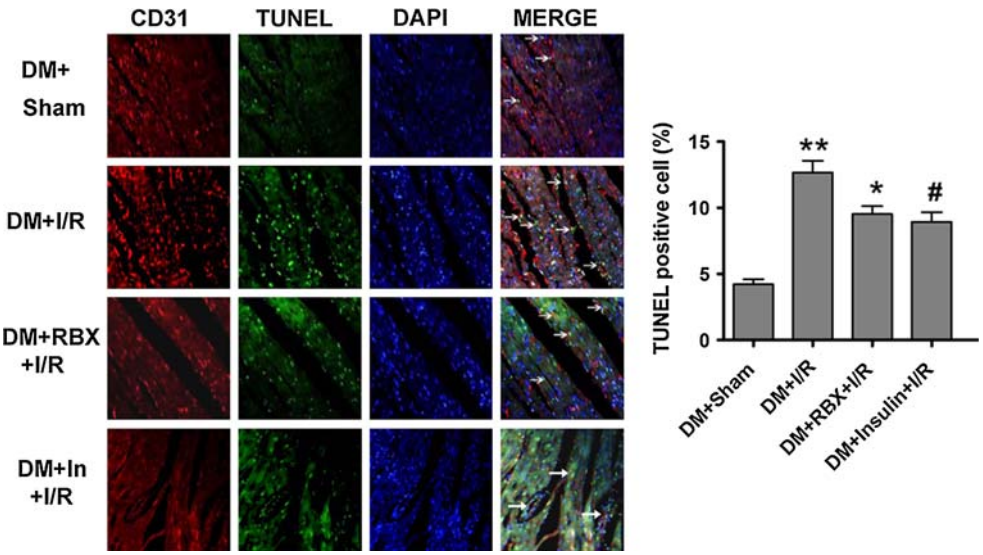

Fig. 2 Apoptosis of CMECs in diabetic rats subjected to sham operation or ischemia reperfusion and receiving different treatments. The merger of green (TUNEL staining) and red (CD31 staining) fluorescent in cells indicated apoptotic CMECs ($n = 6$). The index of apoptosis (AI) was equal to the number of TUNEL-positive CMECs divided by the total CMECs per field. ** $P < 0.01$ vs. DM + Sham, * $P < 0.05$ vs. DM + I/R, $^{\#}$ $P < 0.05$ vs. DM + I/R

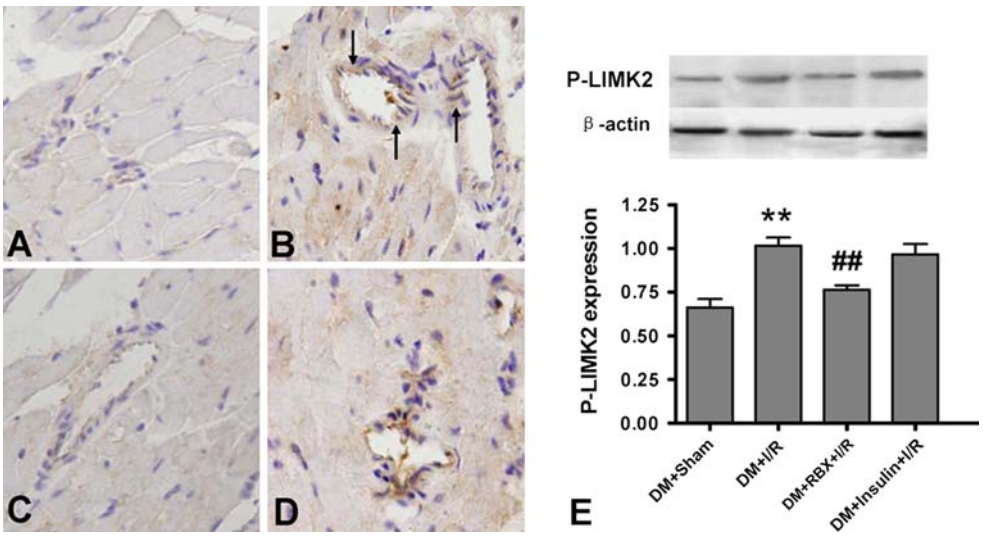

Fig. 3 Phosphor-LIMK2 expression in diabetic rats subjected to sham operation or ischemia reperfusion and receiving different treatments. Phosphor-LIMK2 identified by immunohistochemical staining expressed in sham operated control (**a**), without treatment diabetic rats (**b**), RBX-treated diabetic rats (**c**) and insulin -treated diabetic rats (**d**). Scale bar represents 30 μm. Phosphor-LIMK2 examined with Western blot displayed high expression in diabetic rats and down-regulated by the administration of RBX (**e**) ($n = 8$). ** $P < 0.01$ vs. DM + Sham, $^{\#\#}$ $P < 0.01$ vs. DM + I/R

cofocal microscope (Fig. 4c). Nuclei were stained by DAPI (Fig. 4d).

In order to exclude the influence of osmotic pressure, we observed the effects of high glucose (25 mmol/L) and glucose (5.5 mmol/L) with mannitol (19.5 mmol/L). The results demonstrated that high glucose concentration influenced CMECs apoptosis, however, osmotic control medium containing glucose (5.5 mmol/L) and mannitol (19.5 mmol/L) had no significant effect on apoptosis (6.24 ± 1.42 vs. 5.74 ± 1.38%, $P > 0.01$). CMECs from sham group exhibited very low levels of staining for TUNEL. A significant number of TUNEL-positive CMECs were detected in CMECs after SI/R (13.14 ± 1.72 vs. 5.74 ± 1.38%, $P < 0.01$). However, RBX pretreatment (13.14 ± 1.72 vs. 9.08 ± 1.12%, $P \leq 0.01$) and transfection with PKC-β siRNA (13.14 ± 1.72 vs. 8.74 ± 1.49%, $P \leq 0.01$) significantly decreased the number of TUNEL positive CMECs (Fig. 4e).

RBX pretreatment improved barrier function of CMECs monolayer after SI/R

To examine the effect of SI/R on endothelial barrier function, CMECs were grown to confluence and changes in TER in response to SI/R were monitored (669.2 ± 62.5 Ω vs. 840.2 ± 50.9 Ω, $P < 0.01$). Compared to the no-treatment group,

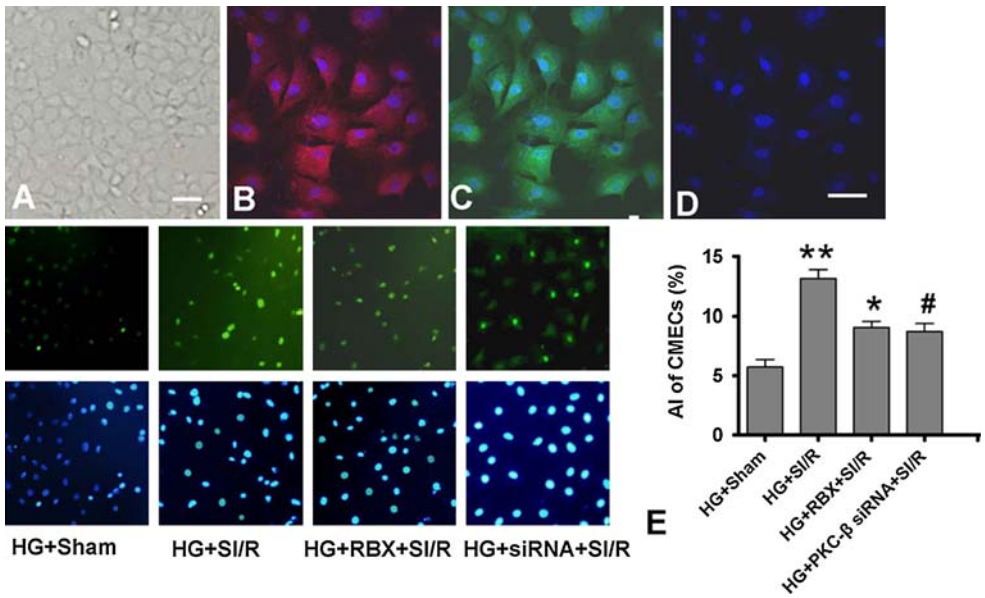

Fig. 4 CMECs identified and apoptosis of CMECs cultured in high-glucose subjected to sham operation or simulated ischemia reperfusion. CMECs were successfully cultured and identified. Confluence of CMECs monolayer: cobble stone appearance (**a**); Scale bar represents 10 μm. Englobing AcLDL in CMECs (**b**); Staining with CD31 (**c**); Staining with DAPI (**d**); Scale bar represents 30 μm. RBX and insulin treatment reduced apoptosis index (AI) of CMECs exposed on high-glucose after simulated ischemia reperfusion (**e**). ** $P < 0.01$ vs. HG +Sham, * $P < 0.05$ vs. HG +SI/R. # $P < 0.05$ vs. HG +SI/R. Representative blots of five independent experiments are shown

RBX (669.2 ± 62.5 Ω vs. 814.3 ± 57.3 Ω, $P \leq 0.01$) and PKC-β siRNA (669.2 ± 62.5 Ω vs. 820.3 ± 68.8 Ω, $P \leq 0.01$) induced a rapid and potent barrier enhancement as detected by increased TER, but there was no significant differences between RBX and PKC-β siRNA (Fig. 5a, b).

FITC-Dextran clearance of CMECs monolayer in high glucose medium subjected to SI/R was increased compared with that in sham group (587.80 ± 33.40 vs. 359.20 ± 22.80, $P < 0.01$). Interestingly, the addition of RBX (432.00 ± 30.83 vs. 587.80 ± 33.40, $P \leq 0.01$) and PKC-β siRNA (414.10 ± 37.28 vs. 587.80 ± 33.40, $P \leq 0.01$) resulted in significant permeability decrease compared with that in the no-treatment group subjected to SI/R (Fig. 5c).

The effects of high glucose (25 mmol/L) and glucose (5.5 mmol/L) with mannitol (19.5 mmol/L) on barrier function was observed. The results demonstrated high glucose concentration influenced CMECs monolayer barrier function, but osmotic control medium containing glucose (5.5 mmol/L) and mannitol (19.5 mmol/L) had no significant effects (680.3 ± 71.3 Ω vs. 669.2 ± 62.5 Ω for TER; 378.10 ± 21.30 vs. 359.20 ± 22.80 for FITC-Dextran clearance, all $P \geq 0.01$).

RBX pretreatment downregulated phosphor-LIMK2 expression and reduced F-actin/G-actin in CMECs after SI/R

Phosphor-LIMK2 expression increased in CMECs subjected to SI/R compared with sham group (1.11 ± 0.09 vs. 0.31 ± 0.09, $P < 0.01$). In contrast, RBX pretreatment (0.68 ± 0.08 vs. 1.11 ± 0.09, $P \leq 0.01$) and transfection with PKC-β siRNA (0.61 ± 0.06 vs. 1.11 ± 0.09, $P \leq 0.01$) significantly lowered phosphor-LIMK2 expression compared with the no-treatment group (Fig. 6e).

F-actin was stained with FITC-phalloidin and highlighted with arrows in Fig. 6 (upper panel). F-actin content of CMECs was found increased in the no-treatment group. However, RBX pretreatment and PKC-β siRNA inhibition reduced F-actin content (Fig. 6a–d). The ratio of F-actin to G-actin in CMECs in no-treatment group after SI/R was significantly higher than that in sham group (10.73 ± 1.32 vs. 6.58 ± 1.34, $P < 0.01$). While, RBX pretreatment (7.32 ± 1.02 vs. 10.73 ± 1.32, $P \leq 0.01$) and PKC-β siRNA inhibition (7.14 ± 1.01 vs. 10.73 ± 1.32, $P \leq 0.01$) have effects to reduce the F-actin to G-actin ratio as compared with high glucose group without pretreatment after SI/R (Fig. 6e–g).

Discussion

The increased risk of death in diabetic patients is related to both microvascular and macrovascular damage. Severe stenosis and poor flow in coronary artery worsens the short and long-term prognoses following acute myocardial infarction (AMI) in diabetic patients compared with non-diabetic patients [24]. Meanwhile, coronary microcirculatory damage is an important factor for the prognosis of

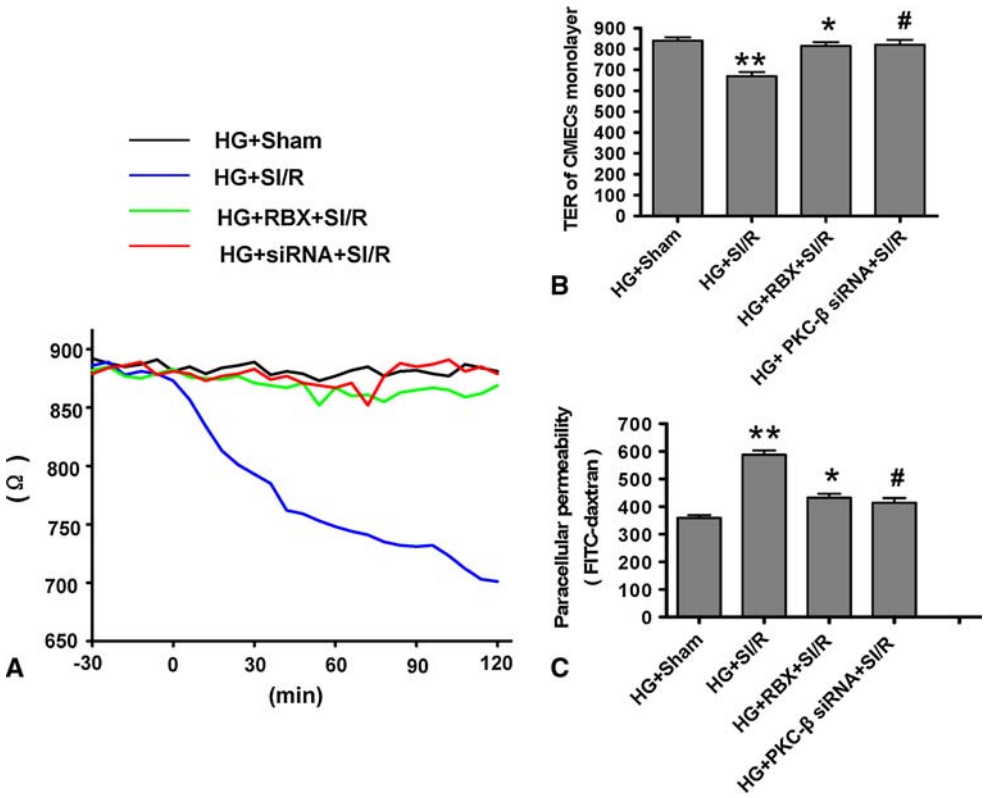

Fig. 5 Transendothelialelectrical resistance (TER) and permeability examination in CMECs cultured in high glucose subjected to sham operation or simulated ischemia reperfusion. RBX and PKC-β siRNA induced barrier enhancement of CMECs monolayer in high glucose medium subjected to simulated ischemia reperfusion (**a, b**). ** $P < 0.01$ vs. HG +Sham, * $P < 0.05$ vs. HG +SI/R, # $P < 0.05$ vs. HG +SI/R. RBX pretreatment and transfection with PKC-β siRNA decreased the permeability of CMECs monolayer in high glucose medium subjected to simulated ischemia reperfusion (**c**). ** $P < 0.01$ vs. HG +Sham, * $P < 0.05$ vs. HG +SI/R, # $P < 0.05$ vs. HG +SI/R. Representative blots of five independent experiments are shown

AMI after revascularization. More importantly, endothelial barrier dysfunction and increased permeability are characteristic changes in coronary microcirculatory damage. Increased microvascular permeability in the coronary system may in large part contribute to myocardium insufficiency and ventricular dysfunction. Aberrations of endothelial barrier function lead to abnormal extravasations of inflammatory factors and result in aggravation of ischemia reperfusion injury.

Our experiments in animals demonstrated that more lanthanum traversed the endothelium, edema and vacuolus were present in diabetic hearts subjected to I/R compare with sham group. Microvascular lesion region was enlarged in diabetic heart under I/R. In contrast, a highly selective PKC-β inhibition through RBX pre-treatment can protect against lanthanum leakage across the endothelium. These results provide direct evidence that RBX can significantly reduce the cardiac microvascular injury in diabetic rats suffering an ischemic insult and that PKC-β dependent signal contributes to the protective effect. In addition, RBX has the similar protective effects as insulin, but insulin did not influence phosphor-LIMK2 expression. These results indicate that insulin's reduction of I/R injury depends on other pathways, not PKC-β dependent signal. In order to further explore its mechanism, we observed the protective effects of RBX on CMECs monolayer barrier function after SI/R in vitro and compared with the effects of transfection with PKC-β siRNA.

Endothelial barrier function is determined by a balance between adhesive forces at intercellular junctions and actin-generated centripetal forces. Increased actin-generated force, loss of adhesive force, or a combination of both may increase paracellular flux of inflammatory factors and macromolecules [25, 26]. Our previous studies also demonstrated I/R can worsen the inflammatory reaction and aggravate cell apoptosis [27, 28]. Centripetal forces are regulated by structural alterations in cytoskeletal filament and actin (F-actin and G-actin) polymerization [29, 30]. The LIMK 2 is serine protein kinases involved in the regulation of actin polymerization. Their activity is regulated by phosphorylation of a threonine residue within the activation loop of the kinase by Rho kinase [31]. Some previous studies have demonstrated phosphorylation of LIM-kinase 2 was modulated by Rho kinase activation.

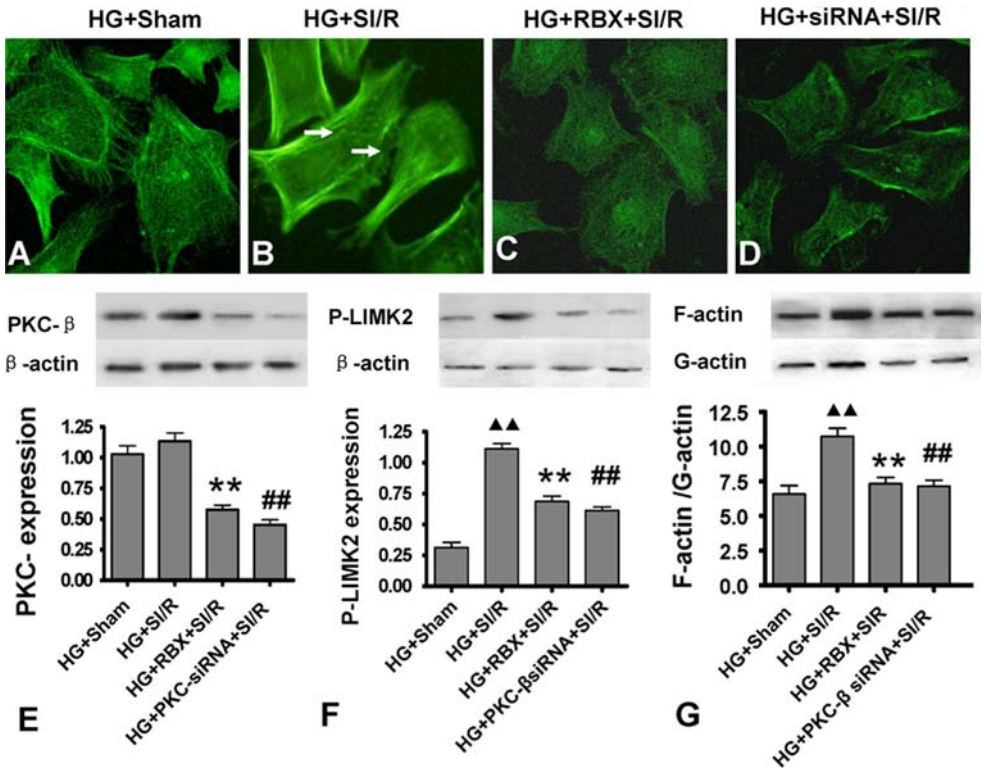

Fig. 6 PKC-β, phosphor-LIMK2 expression and F-actin/G-actin in CMECs cultured in high glucose subjected to sham operation or simulated ischemia reperfusion. F-actin was stained with FITC-phalloidin. Scale bar represents 30 μm (**a–d**). PKC-β depletion induced by PKC-β siRNA was confirmed by Western blot. The pharmacological inhibitor RBX reproduced the same effect as PKC-β silencing reduced protein expression of PKC-β (**e**). ** $P < 0.01$ vs. HG +SI/R, ## $P < 0.01$ vs. HG +SI/R. RBX and PKC-β siRNA pretreatment downregulated phosphor-LIMK2 expression in cultured CMECs after simulated ischemia reperfusion (**f**). ▲▲ $P < 0.01$ vs. HG +Sham, ** $P < 0.01$ vs. HG +SI/R, ## $P < 0.01$ vs. HG +SI/R. RBX PKC-β siRNA pretreatment reduced F-actin/G-actin in CMECs after simulated ischemia reperfusion (**g**). ▲▲ $P < 0.01$ vs. HG +Sham, ** $P < 0.05$ vs. HG +SI/R, ## $P < 0.05$ vs. HG +SI/R. Representative blots of five independent experiments are shown

Vardouli L and colleagues [32] demonstrated transforming growth factor-beta 1 (TGFβ1) induced the phosphorylation of LIMK2 and inhibiting Rho kinase activity completely blocked TGFβ1-induced LIMK2/cofilin phosphorylation and actin polymerization.

In our study, phosphor-LIMK2 in diabetic heart subjected to I/R and cultured CMECs after SI/R significantly augmented. The F-actin/G-actin ratio was paralleled with the increase of phosphorylation of LIM-kinase 2, which indicated actin-generated centripetal forces of an important maintenances agent in normal endothelial barrier was impaired during I/R. Increased F-actin content resulted in loss of equilibrium between actin-generated force and adhesive force. Above series of pathological progress would deteriorate the barrier function of endothelium and encouraged marked elevation of permeability. Those mechanisms possibly help to interpret TER decreased and FITC-Dextran permeability increased in experimental results. We suspect phosphorylation of LIM-kinase 2 primary contributed to cardiac vascular barrier dysfunction during I/R in diabetes. The results of transfection of PKC-β siRNA into CMECs further suggests phosphorylation of LIM-kinase 2 during I/R depended on PKC-β activation in diabetes.

Cell division, motility, and shape determination depend on reorganization of the actin cytoskeleton. Report [33] implicated that inhibition of Rho-kinase can prevent I/R-induced endothelial cell apoptosis and that protective effects of Rho-kinase inhibition are facilitated by prevention of F-actin rearrangement. Several studies demonstrated Rho kinase was activated during ischemia–reperfusion [34, 35]. All these mechanisms may be involved in the mal-effects of Rho kinase activation on the I/R-induced myocardial injury. Our findings suggest that PKC-β activation in diabetes may render cardiac microvascular cells more susceptible to I/R injury by Rho kinase. Phosphorylation of LIM-kinase 2 was likely modulated by up-stream molecular PKC-β-dependent Rho kinase not PKC-β.

We also found apoptosis of CMECs increased accompanying with barrier dysfunction and the actin polymerization. Treatment with RBX or transfection of PKC-β siRNA resulted in a reduction in apoptotic CMECs. This is

consistent with effects on cardiac barrier function, suggesting maintenance of normal cytoskeleton in reperfusion could contribute to the reduction of apoptotic CMECs. Conversely, decreased apoptosis of CMECs helps protect against cardiac barrier dysfunction in I/R progress. Although we showed the beneficial effects of PKC-β inhibition on cardiac microvascular lesion protection likely due to its maintenance of barrier function and anti-apoptotic effect, the specific mechanisms need to be investigated in future studies.

In summary, we demonstrated microvascular I/R injury in diabetes was characterized by loss of normal barrier function of CMECs and increased apoptosis of CMECs. PKC-β activation in diabetes not only modified adhesive force but also render cardiac microvascular cells more susceptible to I/R injury by Rho kinase, which is an injury kinase excessively activation. Phosphor-LIMK2 modulated by PKC-β-dependent Rho kinase was involved in structural alterations in cell barrier function. Furthermore, this condition also resulted in cell gap enlargement, cell edema and cell apoptosis, which further aggravated microvascular I/R injury in diabetic states. Finally, these results indicated PKC-β inhibitor pretreatment for diabetic microvascular complications could be helpful in attenuating the risk of I/R injury. Chronic microvascular complication in diabetes controlled by PKC-β inhibitor ahead of ischemia events also could become a prophylactic agent to severe microvascular I/R injury.

There still existed intriguing points to research in our ongoing study. The detail of PKC-β activation correlated with Rho kinase expression in I/R, which could be detected with co-immunoprecipitation. Actin cytoskeletal dynamics is precisely regulated by a variety of actin-binding proteins involved in polymerization/depolymerization, we can further explore the function of this protein.

Acknowledgments This study was supported by grants from the National Natural Science Foundation of China (NSFC, No. 30770784, 30970845) and Xijing Research Boosting Program (FC, NO. XJZT07Z05, XJZT08Z04).

References

1. Zhang Y, Galloway JM, Welty TK, Wiebers DO, Whisnant JP, Devereux RB et al (2008) Incidence and risk factors for stroke in american indians: the strong heart study. Circulation 118:1577–1584
2. Capes SE, Hunt D, Malmberg K, Gerstein HC (2000) Stress hyperglycaemia and increased risk of death after myocardial infarction in patients with and without diabetes: a systematic overview. Lancet 355:773–778
3. Di Filippo C, Marfella R, Cuzzocrea S, Piegari E, Petronella P, Giugliano D et al (2005) Hyperglycemia in streptozotocin-induced diabetic rat increases infarct size associated with low levels of myocardial HO-1 during ischemia/reperfusion. Diabetes 54:803–810
4. Paulson DJ (1997) The diabetic heart is more sensitive to ischemic injury. Cardiovasc Res 34:104–112
5. Kato M, Dote K, Sasaki S, Ueda K, Goto K, Takemoto H et al (2006) Plain computed tomography for assessment of early coronary microcirculatory damage after revascularization therapy in acute myocardial infarction. Circ J 70:1475–1480
6. Yuan SY, Ustinova EE, Wu MH, Tinsley JH, Xu W, Korompai FL et al (2000) Protein kinase C activation contributes to microvascular barrier dysfunction in the heart at early stages of diabetes. Circ Res 87:412–417
7. Scalia R, Gong Y, Berzins B, Zhao LJ, Sharma K (2007) Hyperglycemia is a major determinant of albumin permeability in diabetic microcirculation: the role of mu-calpain. Diabetes 56:1842–1849
8. Young ME, McNulty P, Taegtmeyer H (2002) Adaptation and maladaptation of the heart in diabetes: part II: potential mechanisms. Circulation 105:1861–1870
9. Scarabelli T, Stephanou A, Rayment N, Pasini E, Comini L, Curello S et al (2001) Apoptosis of endothelial cells precedes myocyte cell apoptosis in ischemia/reperfusion injury. Circulation 104:253–256
10. Das Evcimen N, King GL (2007) The role of protein kinase C activation and the vascular complications of diabetes. Pharmacol Res 55:498–510
11. Bazzoni G, Dejana E (2004) Endothelial cell-to-cell junctions: molecular organization and role in vascular homeostasis. Physiol Rev 84:869–901
12. Zeidan A, Javadov S, Karmazyn M (2006) Essential role of Rho/ROCK-dependent processes and actin dynamics in mediating leptin-induced hypertrophy in rat neonatal ventricular myocytes. Cardiovasc Res 72:101–111
13. Gutterman DD (2002) Vascular dysfunction in hyperglycemia: is protein kinase C the culprit? Circ Res 90:5–7
14. Budhiraja S, Singh J (2008) Protein kinase C beta inhibitors: a new therapeutic target for diabetic nephropathy and vascular complications. Fundam Clin Pharmacol 22:231–240
15. He Z, King GL (2004) Protein kinase Cbeta isoform inhibitors: a new treatment for diabetic cardiovascular diseases. Circulation 110:7–9
16. Beckman JA, Goldfine AB, Gordon MB, Garrett LA, Creager MA (2002) Inhibition of protein kinase Cbeta prevents impaired endothelium-dependent vasodilation caused by hyperglycemia in humans. Circ Res 90:107–111
17. Idris I, Donnelly R (2006) Protein kinase C beta inhibition: a novel therapeutic strategy for diabetic microangiopathy. Diab Vasc Dis Res 3:172–178
18. Ma H, Zhang HF, Yu L, Zhang QJ, Li J, Huo JH et al (2006) Vasculoprotective effect of insulin in the ischemic/reperfused canine heart: role of Akt-stimulated NO production. Cardiovasc Res 69:57–65
19. Xing W, Yan W, Fu F, Jin Y, Ji L, Liu W et al (2009) Insulin inhibits myocardial ischemia-induced apoptosis and alleviates chronic adverse changes in post-ischemic cardiac structure and function. Apoptosis 14:1050–1060
20. Raposo C, Zago GM, da Silva GH, da Cruz Hofling MA (2007) Acute blood-brain barrier permeabilization in rats after systemic *Phoneutria nigriventer venom*. Brain Res 1149:18–29
21. Reffelmann T, Hale SL, Dow JS, Kloner RA (2003) No-reflow phenomenon persists long-term after ischemia/reperfusion in the rat and predicts infarct expansion. Circulation 108:2911–2917
22. Chiang ET, Camp SM, Dudek SM, Brown ME, Usatyuk PV, Zaborina O et al (2009) Protective effects of high-molecular weight polyethylene glycol (PEG) in human lung endothelial cell barrier regulation: role of actin cytoskeletal rearrangement. Microvasc Res 77:174–186

23. Sun X, Shikata Y, Wang L, Ohmori K, Watanabe N, Wada J et al (2009) Enhanced interaction between focal adhesion and adherens junction proteins: involvement in sphingosine 1-phosphate-induced endothelial barrier enhancement. Microvasc Res 77:304–313
24. Harjai KJ, Stone GW, Boura J, Mattos L, Chandra H, Cox D et al (2003) Comparison of outcomes of diabetic and nondiabetic patients undergoing primary angioplasty for acute myocardial infarction. Am J Cardiol 91:1041–1045
25. Baldwin AL, Thurston G (2001) Mechanics of endothelial cell architecture and vascular permeability. Crit Rev Biomed Eng 29:247–278
26. Bazzoni G, Dejana E (2001) Pores in the sieve and channels in the wall: control of paracellular permeability by junctional proteins in endothelial cells. Microcirculation 8:143–152
27. Gao HK, Yin Z, Zhou N, Feng XY, Gao F, Wang HC (2008) Glycogen synthase kinase 3 inhibition protects the heart from acute ischemia-reperfusion injury via inhibition of inflammation and apoptosis. J Cardiovasc Pharmacol 52:286–292
28. Wang HC, Zhang HF, Guo WY, Su H, Zhang KR, Li QX et al (2006) Hypoxic postconditioning enhances the survival and inhibits apoptosis of cardiomyocytes following reoxygenation: role of peroxynitrite formation. Apoptosis 11:1453–1460
29. Yuan SY (2002) Protein kinase signaling in the modulation of microvascular permeability. Vascul Pharmacol 39:213–223
30. Yuan SY, Wu MH, Ustinova EE, Guo M, Tinsley JH, De Lanerolle P et al (2002) Myosin light chain phosphorylation in neutrophil-stimulated coronary microvascular leakage. Circ Res 90:1214–1221
31. Bernard O (2007) Lim kinases, regulators of actin dynamics. Int J Biochem Cell Biol 39:1071–1076
32. Vardouli L, Moustakas A, Stournaras C (2005) LIM-kinase 2 and cofilin phosphorylation mediate actin cytoskeleton reorganization induced by transforming growth factor-beta. J Biol Chem 280:11448–11457
33. van der Heijden M, Versteilen AM, Sipkema P, van Nieuw Amerongen GP, Musters RJ, Groeneveld AB (2008) Rho-kinase-dependent F-actin rearrangement is involved in the inhibition of PI3-kinase/Akt during ischemia-reperfusion-induced endothelial cell apoptosis. Apoptosis 13:404–412
34. Bao W, Hu E, Tao L, Boyce R, Mirabile R, Thudium DT et al (2004) Inhibition of Rho-kinase protects the heart against ischemia/reperfusion injury. Cardiovasc Res 61:548–558
35. Yada T, Shimokawa H, Hiramatsu O, Kajita T, Shigeto F, Tanaka E et al (2005) Beneficial effect of hydroxyfasudil, a specific rho-kinase inhibitor, on ischemia/reperfusion injury in canine coronary microcirculation in vivo. J Am Coll Cardiol 45:599–607